

NISTIR 89-4052



Calculation of the Flow Through a Horizontal Ceiling/Floor Vent

Leonard Y. Cooper

U.S. DEPARTMENT OF COMMERCE
National Institute of Standards and Technology
(Formerly National Bureau of Standards)
National Engineering Laboratory
Center for Fire Research
Gaithersburg, MD 20899

March 1989

Sponsored in part by:
Naval Research Laboratory
Washington, DC 20375

NISTIR 89-4052

Calculation of the Flow Through a Horizontal Ceiling/Floor Vent

Leonard Y. Cooper

U.S. DEPARTMENT OF COMMERCE
National Institute of Standards and Technology
(Formerly National Bureau of Standards)
National Engineering Laboratory
Center for Fire Research
Gaithersburg, MD 20899

March 1989



National Bureau of Standards became the National Institute of Standards and Technology on August 23, 1988, when the Omnibus Trade and Competitiveness Act was signed. NIST retains all NBS functions. Its new programs will encourage improved use of technology by U.S. industry.

Sponsored in part by:
Naval Research Laboratory
Washington, DC 20375

U.S. DEPARTMENT OF COMMERCE
Robert Mosbacher, Secretary
Ernest Ambler, Acting Under Secretary
for Technology
NATIONAL INSTITUTE OF STANDARDS
AND TECHNOLOGY
Raymond G. Kammer, Acting Director

TABLE OF CONTENTS

	Page
LIST OF FIGURES.....	iv
ABSTRACT.....	1
1. Introduction.....	2
2. A Basic Problem with the Standard Vent-Flow Model.....	3
3. A Model for Exchange Flow When $\Delta p = 0$ and Minimum-Exchange-Flow Conditions for Non-Zero Δp	4
4. An Estimate for $ \Delta p_{\text{FLOOD}} $ and for V_{EX} when $0 < \Delta p \leq \Delta p_{\text{FLOOD}} $	6
5. VENTCL - An Algorithm for Flow Through Horizontal Ceiling/Floor Vents.....	11
6. Example Application of VENTCL: Steady-State Rate-of-Burning in a Ceiling-Vented Space.....	11
7. Acknowledgements.....	14
8. References.....	15
9. Nomenclature.....	16

LIST OF FIGURES

	Page
Figure 1.	The basic horizontal-vent configuration..... 18
Figure 2.	The standard vent-flow model for horizontal vents..... 19
Figure 3.	The volume-flow rate components $V_{TOP,ST}$ and V_{EX} for unstable Figure-1 configurations, $\Delta\rho > 0$, plotted as functions of Δp 20
Figure 4.	Sketch of the experimental set-up of Mercer and Thompson [9]..... 21
Figure 5.	Plots of the Mercer and Thompson [9] data for $\theta = 0$ (horizontal), 45, 60, and 90°..... 22
Figure 6.	The vertical-vent configuration used to calculate minimum totally-purging flow rates..... 23
Figure 7.	Configuration of a ceiling-vented room with a fire..... 24
Figure 8.	Plots of $ \Delta p/\Delta p_{FLOOD} $, $Q/[(1 - \mu/\mu_{AMB})\mu_{AMB}C_{OXYGEN}\rho_{AMB}(gA_V^{5/2})^{1/2}]$ $= Q_{MAX}/[(1 - \mu_{EXTINCTION}/\mu_{AMB})\mu_{AMB}C_{OXYGEN}\rho_{AMB}(gA_V^{5/2})^{1/2}]$ as functions of T/T_{AMB} for the configuration of Figure 7... 25

CALCULATION OF THE FLOW THROUGH A HORIZONTAL CEILING/FLOOR VENT

by

Leonard Y. Cooper
Center for Fire Research
National Institute of Standards and Technology
Gaithersburg, MD 20899

Abstract

Calculation of the flow through a horizontal vent located in a ceiling or floor of a multi-room compartment is considered. It is assumed that the environments of the two, vent-connected spaces near the elevation of the vent are of arbitrary relative buoyancy and cross-vent pressure difference, Δp . An anomaly of the standard vent flow model, which uses Δp to predict stable uni-directional flow according to Bernoulli's equation (i.e., flow rate is proportional to $\Delta p^{1/2}$), is discussed. The problem occurs in practical vent configurations of unstable hydrostatic equilibrium, where, for example, one gas overlays a relatively less-dense gas, and where $|\Delta p|$ is relatively small. In such configurations the cross-vent flow is not uni-directional. Also, it is not zero at $\Delta p = 0$. Previously published experimental data on a variety of related flow configurations are used to develop a general flow model which does not suffer from the standard model anomaly. The model developed leads to a uniformly valid algorithm, called VENTCL, for horizontal vent flow calculations suitable for general use in zone-type compartment fire models. Based on an assumption of total consumption of net oxygen flow rate, the algorithm is used in an example application where steady-state rate-of-burning in a ceiling-vented room is estimated as a function of room temperature, vent area, and oxygen concentration.

Keywords: algorithms; building fires; compartment fires; computer models; computer programs; fire modeling; pressure differential; pressure effects; vent flow; zone modeling.

1. Introduction

Consider an instant of time during the simulation of a multi-room compartment fire environment. This paper develops an algorithm for calculating quasi-steady characteristics of the flow through a horizontal vent located in a ceiling or floor of the compartment where the environments of the two, vent-connected spaces near the elevation of the vent are of arbitrary relative buoyancy. With such an algorithm it would be possible to calculate the effect of ceiling-vent flows on dynamic changes in the environments of the two connected spaces and throughout the entire multi-room facility.

Throughout this work it is assumed that in each space, near the vent elevation, but away from the vent flow itself, the environment is relatively quiescent with pressure well-approximated by the uniform pressure field which would be derived from hydrostatic momentum considerations. This assumption would be satisfied typically if the area of the vent, A_v , is small compared to the plan area of either the upper or lower space.

Designate the two spaces being connected by the vent as the top and bottom spaces. Subscripts BOT and TOP will always refer to conditions in the bottom and top spaces, respectively. Refer to Figure 1 and assume that the environment in each of the two spaces is known. The properties of the environment which are critical in the determination of the characteristics of the flow through the vent are the densities, ρ_{TOP} and ρ_{BOT} , and the pressure difference, Δp , defined by

$$\Delta p = P_{BOT} - P_{TOP} \quad (1)$$

where P_{BOT} and P_{TOP} are the hydrostatic pressures at the vent elevation. In typical fire scenarios Δp is small compared to P_{BOT} and P_{TOP} . If such is not the case, e.g., if one of the spaces is near-hermetically sealed and is a space of fire origin, then the vent flow will also depend on one of P_{BOT} or P_{TOP} .

The objective of this work is to develop a model to predict the flow through the vent for arbitrary values of ρ_{TOP} , ρ_{BOT} , and Δp (or P_{BOT} and P_{TOP}).

There exists a simple, effective model for estimating the flow through both horizontal and vertical vents which is used uniformly in modeling compartment fire phenomena. The model (which will be referred to here as the standard vent-flow model) uses Bernoulli's equation and an appropriate orifice-like jet contraction coefficient to compute a uniform velocity and then the volumetric- or mass-flow-rate through the vent. In the case of vertical vents, the cross-vent hydrostatic pressure difference required in Bernoulli's equation varies with elevation over the vent area. The details of the total flow calculation for vertical vents involves integration of elevation-dependent mass flux across the area. A numerical calculation for an arbitrary vent-area shape poses no practical problem. For a rectangular vertical vent the calculation has been obtained in closed form (see, e.g., Emmons [1]) and the result of this is used commonly in room fire models.

In compartment fire modeling, the above-mentioned vent-flow model was first proposed and used by Thomas, et al [2] to treat problems of ceiling venting of building spaces which are "freely" ventilated with make-up air from side vents. The model has found much use over the last few decades in the analysis of roof venting problems. Recently, it has been used by Cooper [3] and Hinkley [4] to model the interactions of ceiling vents, smoke layering, and the response of near-ceiling-mounted fusible links in dynamic fire environments.

2. A Basic Problem with the Standard Vent-Flow Model

As suggested above, the standard vent-flow model is at its simplest in the horizontal, ceiling-vent application, where Δp and velocity are predicted to be uniform over the vent area. Therefore, in a sense it is ironic that in this application, and not in the somewhat-more-complicated vertical-vent application, the model breaks down for an important, and to-date untreated class of ceiling-vented fire scenario.

The basic problem can be illustrated with the use of Figure 1. Assume that $\rho_{TOP} > \rho_{BOT}$. This occurs when the vent separates a relatively high-temperature, small-density environment at the bottom (for example, the bottom space contains a fire or is near to a space-of-fire-origin) from a relatively-cool, high-density environment at the top. According to the standard, vent-flow model, the flow through the vent for different values of Δp is given by

$$\text{For arbitrary } \Delta\rho = \rho_{TOP} - \rho_{BOT}: \quad (2)$$

$$V_{BOT,ST} = C_D A_V |2\Delta p / \rho_{BOT}|^{1/2}, \quad V_{TOP,ST} = 0 \quad \text{if } \Delta p > 0 \quad (3)$$

$$V_{BOT,ST} = 0, \quad V_{TOP,ST} = 0 \quad \text{if } \Delta p = 0 \quad (4)$$

$$V_{BOT,ST} = 0, \quad V_{TOP,ST} = C_D A_V |2\Delta p / \rho_{TOP}|^{1/2} \quad \text{if } \Delta p < 0 \quad (5)$$

where $V_{BOT,ST}$ and $V_{TOP,ST}$ are the volume-flow-rates through the vent from the bottom space to the top space and from the top space to the bottom space, respectively, A_V is the vent area, and C_D is the flow coefficient. The above flows are illustrated in Figure 2. Note that the standard model always yields unidirectional flow through the vent, where the flow direction is determined by the sign of Δp , i.e., $V_{BOT,ST}$ and $V_{TOP,ST}$ are never both non-zero.

The above flow description seems reasonable, except for one problem which is highlighted by Eq. (4) and Figure 2(b), namely, the prediction of a state of stable hydrostatic equilibrium corresponding to a zero exchange flow when $\Delta p = 0$. The prediction is wrong! Indeed, the hydrostatic state associated with the assumed configuration is not one of stable equilibrium and non-zero, time-dependent, exchange flows between the spaces are to be expected.

The breakdown of the standard model in the conjectured configuration would be illustrated clearly by the following "bottle-emptying" experiment:

Consider a paper-capped narrow-necked bottle filled with liquid. The bottle is carefully turned upside-down and the paper is removed quickly. For this situation the standard vent-flow model predicts a zero-flow solution with the bottle remaining filled with the liquid, with a low-to-zero (vacuum) state at the top of the column of liquid in the bottle, and with $\Delta p = 0$ across the free-boundary at the vent-like mouth of the bottle. It is evident that the bottle will empty and that here, as in the above configuration, the standard model is invalid.

The problem of the standard model, as applied to horizontal-vent scenarios, is embodied in the uniform prediction of a uni-directional flow. Hydrostatic configurations where an open horizontal vent separates gas or liquid in the top space from a less-dense gas or liquid in the bottom space are always unstable and a uni-directional flow prediction will always be invalid under conditions of "near-zero" Δp . Instead of uni-directional flow, it is evident that a two-directional flow, an exchange flow, develops where the top and bottom spaces exchange their contents with one another. The rate-of-exchange depends on the earlier-identified critical characteristics of the problem.

Beside the above experimental "proof" of the standard-model anomaly, a theoretical study of the relevant fluid-dynamic instability by Taylor [6] is also available. Epstein [7] used this study to guide his analysis of the quasi-steady characteristics of the exchange-flow problem under $\Delta p = 0$ conditions. He then used the results of this analysis to establish a means of correlating his data from a set of salt-water/fresh-water exchange-flow experiments and data of Brown [8] from a set of analogous hot-air/cold-air exchange-flow experiments.

It is the purpose of the paper to propose a fully-general, modified ceiling-vent flow algorithm which corrects the above anomaly of the standard model.

Unless noted otherwise, throughout this work only quasi-steady features of the flows being studied will be discussed and analyzed. Thus, even when the flows being modeled are strongly time-dependent, it is assumed tacitly that time scales which characterizes their fluctuations are relatively small i.e., it is assumed that meaningful average flow characteristics could be established, in principle, with integrals over time intervals which are relatively small compared to the characteristic times of the problems of interest.

3. A Model for Exchange Flow When $\Delta p = 0$ and Minimum-Exchange-Flow Conditions for Non-Zero Δp

Since the standard vent-flow model is not generally adequate, assume that the correct vent flow, V_{TOP} and V_{BOT} , can be predicted by a sum of the standard model flow components of Eqs. (2)-(5) and an exchange-flow component, V_{EX} , to be determined. Thus,

$$V_{TOP} = V_{TOP,ST} + V_{EX} \quad (6)$$

$$V_{BOT} = V_{BOT,ST} + V_{EX}$$

When the density configurations do not lead to an unstable hydrostatic configuration the standard model is valid. In particular,

$$V_{EX} = 0 \text{ for arbitrary } \Delta p \text{ if } \rho_{TOP} \leq \rho_{BOT} \quad (7)$$

For the Figure 1 scenario under the conditions $\rho_{TOP} > \rho_{BOT}$ and $\Delta p = 0$, Epstein [7] proposes the following for the exchange flow through horizontal circular vents:

$$V_{EX} = 0.055[g\Delta\rho D^5/\bar{\rho}]^{1/2} \text{ if } \rho_{TOP} > \rho_{BOT} \text{ and } \Delta p = 0 \quad (8)$$

where D is the diameter of the vent, g is the acceleration of gravity, and

$$\bar{\rho} = (\rho_{TOP} + \rho_{BOT})/2 \quad (9)$$

In terms of the vent area, $A_V = \pi D^2/4$, Eq. (8) can be written as

$$V_{EX} = 0.10[g\Delta\rho A_V^{5/2}/\bar{\rho}]^{1/2} \text{ if } \rho_{TOP} > \rho_{BOT} \text{ and } \Delta p = 0 \quad (8')$$

To the accuracy indicated, the data of Epstein [7] suggests that V_{EX} for square vents can also be predicted by Eq. (8').

If $|\Delta p|$ is increased from zero, but is not too large, a non-zero V_{EX} will continue to persist. If $|\Delta p|$ exceeds some critical value, $|\Delta p_{FLOOD}|$, to be determined, than V_{EX} will become identically zero. Thus,

$$V_{EX} = 0 \text{ if } \rho_{TOP} > \rho_{BOT} \text{ and } |\Delta p| > |\Delta p_{FLOOD}| \quad (10)$$

In accordance with Eq. (6), the flow through the vent will then be simulated accurately by the standard model.

With the unstable density configuration, there will be some flow exchanges, i.e., non-zero V_{EX} , between the environments of the two spaces if $|\Delta p| < |\Delta p_{FLOOD}|$. Alternatively, if $|\Delta p| > |\Delta p_{FLOOD}|$ is maintained then in accordance with Eq. (10) there will be no exchange-flow. Under the latter circumstances the flow through the vent will be uni-directional and, following the standard vent-flow model, it will lead to a total purging of the

environment of one of the spaces, determined by the sign of Δp , from that of the other.

For the unstable density configuration of Figure 1, the components of V_{TOP} , $V_{TOP,ST}$ and V_{EX} , are depicted in Figure 3 according to the above flow model. Reflecting the $V_{TOP,ST}$ plot of Figure 3 in the V axis leads to an analogous plot for $V_{BOT,ST}$. Note that while the functional dependence of V_{EX} on Δp is unknown, it is assumed here that the simple linear dependence indicated in the figure leads to a reasonable model of the flow phenomena being studied.

In the context of the present discussion, the change from maximum exchange flow rate at $|\Delta p| = 0$ to minimum totally-purging, uni-directional flow rate at $|\Delta p| = |\Delta p_{FLOOD}|$ is analogous to the phenomena one would observe during a variation of the above bottle-emptying experiment where a hole is introduced at the top end of the bottle, opposite from the end with the narrow-neck opening. As the area of this hole is increased from zero, the emptying process involves: a decrease of Δp from zero; a corresponding increase in $V_{TOP,ST}$ from zero according to Eq. (5); and a decrease in V_{EX} from its maximum, $\Delta p = 0$ value. Depending on the height of the fluid in the bottle and on the size of the bottle neck, further increases in hole size may lead to $|\Delta p| \geq |\Delta p_{FLOOD}|$ and to a uni-directional flow with zero exchange flow rate per Eq. (10).

The "purging" terminology in the above discussion is taken from the technology of nuclear reactor safety. There it is important to be able to predict conditions where totally-purging flows will give way to flows involving non-zero exchange flows between reactor vessels and outside fluid sources. For the Figure 1-configuration of present interest, research results motivated by that technology will be used here to determine an estimate for $|\Delta p_{FLOOD}|$. With $|\Delta p_{FLOOD}|$ in hand, V_{EX} will be obtained in a manner consistent with the plot of Figure 3.

4. An Estimate for $|\Delta p_{FLOOD}|$ and for V_{EX} when $0 < |\Delta p| \leq |\Delta p_{FLOOD}|$

Conditions for steady, near-totally-purging flow between spaces connected by a relatively long, straight, inclined, circular pipe of diameter D have been determined experimentally by Mercer and Thompson [9]. The configuration for their experiments is sketched in Figure 4. The bottom and top tanks contained fresh water and a relatively-dense salt-water solution, respectively. Each experimental run involved a steady uni-directional flow of salt-water, from the outlet of the top tank, of measured volume-flow-rate, V_{MEAS} . For small enough V_{MEAS} and at the entrance to the lower tank, a limited-length wedge of lower-tank fresh water was observed flowing back into the pipe. If V_{MEAS} was decreased by decreasing the pressure head, then W , the length of the flow wedge, was increased. W/D was taken as a measure of the purging effectiveness associated with the dimensionless flow rate, $V_{MEAS}/[g\Delta\rho D^5/\rho_{TOP}]^{1/2}$. For the experimental configuration of [9], a minimum totally-purging value of V_{MEAS} is defined here as a flow rate which would lead to $W = 0$ exactly. Larger flow rates would lead to continued total purging from the pipe of lower-tank fresh water. In general, the W/D -vs- $V_{MEAS}/[g\Delta\rho D^5/\rho_{TOP}]^{1/2}$ data of [9] were well-correlated as a strong function of pipe inclination, θ . Data reported for $\theta =$

0, 16, 30, 45, 60, 75 and 90° included W/D values which ranged from 0.7-2.2 at the low end to 10.0-15.8 at the high end. Data from [9] for $\theta = 0$ (horizontal), 45, 60, and 90° are reproduced in Figure 5.

For the present application, primary interest in the data of a reference-[9] type of experiment would be in flow rates which lead to limiting small values of W/D. Such flow rates would be analogous to the minimum values of V_{TOP} or V_{BOT} of Figure 2(a) or Figure 2(c), respectively, required for totally-purging, uni-directional vent flow. Note that the analogy between the pipe flow and the vent flow is not perfect since, in the reference-[9] experiments a $W = 0$ flow would enter the lower tank as a fully-developed or nearly-fully-developed pipe flow and this is different than a Figure 2(a) or 2(c) orifice-type of vent-entry flow.

As mentioned, in the experimental study of [9] W was found to be a strong function of pipe inclination. However, when extrapolating the data presented there to limiting-small values of W/D, significant dependence on inclination appears to disappear.¹ (Although the flow rate for the $W/D = 0$ limit is of particular importance here, it was not investigated specifically in [9]. For this reason, the limiting-condition result can only be obtained by extrapolation of the reference [9] data.) This is true for all θ configurations studied in [9], and can be seen in Figure 5 for $\theta = 0, 45,$ and 60° . Thus, a single value of $V_{MEAS}/[g\Delta\rho D^5/\rho_{TOP}]^{1/2}$ appears to be associated with minimum totally-purging conditions, i.e.,

For arbitrary pipe orientations:

$$\lim_{W/D \rightarrow 0} V_{MEAS}/[g\Delta\rho D^5/\rho_{TOP}]^{1/2} = F(\text{shape}) \quad (11)$$

where, for the circular-pipe experiments of [9], $F(\text{shape}) = F(\text{circular pipe})$ is approximately 0.51-0.63 (i.e., relative to the abscissas of Figure 5 and of other plots of [9], $\lim_{W/D \rightarrow 0} [4/\pi]V_{MEAS}/[g\Delta\rho D^5/\rho_{TOP}]^{1/2}$ is approximately 0.65-0.80).

For the present study of vent flows this latter result is very important. Thus, it is reasonable to expect that exchange-flow phenomena for vents at different vent angles are analogous to exchange-flow phenomena for pipes (at

¹Compared to all other data reported in [9] the most interesting data for the present purpose, that acquired for $\theta = 90^\circ$, exhibited highly-unsteady W behavior. In difference to all other W measurements reported in [9], the W measurements for this case are reported as average, rather than peak values. For this reason, extrapolation of reported W vs V_{MEAS} data to $W = 0$ (leading to $[4/\pi]V_{MEAS}/[g\Delta\rho D^5/\rho_{TOP}]^{1/2} \approx 0.3$, as can be seen in Figure 5) can not be expected to yield the desired minimum totally-purging limit, and the $\theta = 0$ data are not useful in the present considerations.

the wedge-flow, outlet end) at different pipe angles. For example, just as the $W/D = 0$ or minimum totally-purging values of $V_{MEAS}/[g\Delta\rho D^5/\rho_{TOP}]^{1/2}$ tend to be relatively independent of orientation for the circular pipe flows of [9], so it is reasonable to assume that the minimum totally-purging values of $V_{TOP}/[g\Delta\rho D^5/\rho_{TOP}]^{1/2}$ or $V_{BOT}/[g\Delta\rho D^5/\rho_{BOT}]^{1/2}$ for flows through a vent of specified shape would tend to be relatively independent of vent orientation. Regarding vent orientation, the vent configuration of Figure 1 would be associated with the $\theta = 90^\circ$ pipe angle and the vent orientation of Figure 6 with the $\theta = 0^\circ$ pipe angle. Minimum totally-purging flow rates for vents will be designated as $V_{TOP,FLOOD}$ and $V_{BOT,FLOOD}$ when flows are from the top and bottom, respectively. Corresponding to Eq. (11), the above assumption can be expressed as

For arbitrary vent orientation:

$$\left. \begin{aligned} V_{TOP,FLOOD}/[g\Delta\rho D^5/\rho_{TOP}]^{1/2} &= \lim_{V_{BOT} \downarrow 0} V_{TOP}/[g\Delta\rho D^5/\rho_{TOP}]^{1/2} \\ V_{BOT,FLOOD}/[g\Delta\rho D^5/\rho_{BOT}]^{1/2} &= \lim_{V_{TOP} \downarrow 0} V_{BOT}/[g\Delta\rho D^5/\rho_{BOT}]^{1/2} \end{aligned} \right\} = f(\text{shape}) \quad (12)$$

where D is a characteristic dimension of a particular vent shape of interest.

The assumption of Eq. (12) will be adopted here. Having done so, the minimum totally-purging flow rate for the Figure 6 configuration will be obtained by the well-known model for flow through a vertical vent [1]. As a result of Eq. (12) this flow rate will be identical for all possible vent orientations, including the horizontal, Figure-1 orientation of present interest. Then, using the standard vent-flow model of Eqs. (2)-(5) for horizontal vents, the value of Δp required to produce the newly-available minimum totally-purging flow rate will be obtained. By definition, this Δp will be identical to Δp_{FLOOD} .

For the vertical vent of Figure 6, near-totally-purging conditions occur with a limiting-small positive V_{TOP} flow when the horizontal neutral plane (i.e., the elevation where $\Delta p = 0$) is exactly at the top of the vent, $z = D$, and with a limiting-small positive V_{BOT} flow when the horizontal neutral plane is exactly at the base of the vent, $z = 0$. With this in mind, the flow rates $V_{TOP,FLOOD}$ and $V_{BOT,FLOOD}$ for vertical vents can be obtained using standard vertical-vent flow calculations. Using the standard vertical-vent flow model [1], it can be shown that for vertical vent shapes which are symmetric about a horizontal axis, the flow rates can be obtained from

$$[V_{TOP,FLOOD}, V_{BOT,FLOOD}] = (g\Delta\rho D^5 / \rho_{FLOOD})^{1/2} C_D C_{SHAPE} \quad (13)$$

$$C_{SHAPE} = 2^{1/2} \int_0^1 (z/D)^{1/2} (w/D) d(z/D) \quad (14)$$

where $w(z)$ is the width of the vent, D is the depth of the vent, and ρ_{FLOOD} is ρ_{TOP} or ρ_{BOT} depending on whether the totally-purging flow is due to a non-zero V_{TOP} or V_{BOT} , respectively, i.e.,

$$\rho_{FLOOD} = \begin{cases} \rho_{TOP} & \text{if } \Delta p < 0 \\ \rho_{BOT} & \text{if } \Delta p > 0 \end{cases} \quad (15)$$

Using Eq. (14), the following results are obtained for circular vents, and rectangular vents of width, w , depth, D , and with sides parallel to the horizontal:

$$C_{SHAPE} = \begin{cases} (2^{7/2}/15) = 0.754 & \text{for a circle} \\ (2^{3/2}/3)(w/D) = 0.942(w/D) & \text{for a rectangle} \end{cases} \quad (16)$$

Note that for circular vents with $C_D = 0.68-1.0$ the Eq. (13)-(16) result for $V_{TOP,FLOOD}/[g\Delta\rho D^5/\rho_{TOP}]^{1/2}$ is comparable to the extrapolated, $W/D = 0$ limit of the reference-[9] data for $V_{MEAS}/[g\Delta\rho D^5/\rho_{TOP}]^{1/2}$, i.e., compare $0.754(0.68) = 0.45$ or $0.754(1.0) = 0.754$ to the range $0.51-0.63$. The favorable comparison of these two results adds support to the analogy between the reference-[9] experiments and vent flows of present interest.

As a point of information, the above results for an unstable Figure-1 configuration also provide a comparison between the total-flow rate of Eq. (13) for minimum totally-purging vertical vent flows and the Eq. (8) value for $V_{EX}(\Delta p=0)$. Thus, for circular vents and for purging flows from the top or bottom, the ratio of the former to the latter volume-flow rate is found to be

$$V_{TOP,FLOOD}/V_{EX}(\Delta p=0) = (0.754/0.055)C_D [(1 + \rho_{TOP}/\rho_{BOT})/(2\rho_{TOP}/\rho_{BOT})]^{1/2} \quad (17)$$

$$V_{BOT,FLOOD}/V_{EX}(\Delta p=0) = (0.754/0.055)C_D [(1 + \rho_{TOP}/\rho_{BOT})/2]^{1/2} \quad (18)$$

From Eq. (17) it is seen that for $\Delta p \leq 0$, which leads to purging flows from the top, the ratio of the flow rates is approximately $(0.754/0.055)C_D = 14.C_D$ when $\rho_{TOP}/\rho_{BOT} \approx 1$ and decreases monotonically with increasing ρ_{TOP}/ρ_{BOT} to the asymptotic value $(0.754/0.055)C_D/2^{1/2} = 10.C_D$ when $\rho_{TOP}/\rho_{BOT} \gg 1$. From

Eq. (18) it is seen that for $\Delta p \geq 0$, which leads to purging flows from the bottom, the ratio of the flow rates is also $14.C_D$ when $\rho_{TOP}/\rho_{BOT} \approx 1$, but increases monotonically with increasing ρ_{TOP}/ρ_{BOT} to approximately $10.C_D(\rho_{TOP}/\rho_{BOT})^{1/2}$ when $\rho_{TOP}/\rho_{BOT} \gg 1$. The latter result for large ρ_{TOP}/ρ_{BOT} relates, for example, to the Figure-1 configuration with a liquid at the top and a gas at the bottom. The result indicates properly that purging from the bottom would require a minimum-volume-flow rate of the gas (and an associated minimum $\Delta p = \Delta p_{FLOOD}$, to be determined below), far in excess of the exchange-volume-flow rate that would exist under the $\Delta p = 0$ condition, the ratio of the two flow rates being proportional to $(\rho_{TOP}/\rho_{BOT})^{1/2} \gg 1$.

The minimum totally-purging flow-rate values of Eq. (13) are now equated to the flow-rate values of Eqs. (2)-(5), where in the latter equations Δp is replaced by Δp_{FLOOD} . This leads to the solution for $|\Delta p_{FLOOD}|$

$$|\Delta p_{FLOOD}| = C_{SHAPE}^2 g \Delta \rho D^5 / (2A_V^2) \quad (19)$$

For the rectangular shape, the side length, D, should be chosen to be the longer of the two sides since that yields the largest value for $|\Delta p_{FLOOD}|$ and, therefore, the value that would guarantee the desired minimum totally-purging result.

With the value of $|\Delta p_{FLOOD}|$ in hand, it is now possible to construct the model for V_{EX} when non-zero exchange-flows are expected. As indicated in Figure 3, it is assumed that in the range $0 < |\Delta p| \leq |\Delta p_{FLOOD}|$, V_{EX} varies linearly with Δp , going from its maximum Eq. (8) value at $\Delta p = 0$ to zero at $\Delta p = \pm |\Delta p_{FLOOD}|$.

$$V_{EX} = \begin{cases} V_{EX,MAX} (1 - |\Delta p|/|\Delta p_{FLOOD}|) & \text{if } \Delta p > 0 \text{ and } |\Delta p|/|\Delta p_{FLOOD}| < 1 \\ 0 & \text{otherwise} \end{cases} \quad (20)$$

In the above, $|\Delta p_{FLOOD}|$ is calculated from Eq. (19) where, according to Eqs. (8), (8'), and (10), $V_{EX,MAX}$ is calculated from

$$V_{EX,MAX} = 0.055 [2g\Delta\rho D^5 / (\rho_{TOP} + \rho_{BOT})]^{1/2} \text{ for circular vents, or} \quad (21)$$

$$V_{EX,MAX} = 0.10 [2g\Delta\rho A_V^{5/2} / (\rho_{TOP} + \rho_{BOT})]^{1/2}$$

for circular or square vents

and where special considerations, and possibly new reference [7]-type exchange-flow experiments may be required to establish $V_{EX,MAX}$ for other shapes.

5. VENTCL - An Algorithm for Flow Through Horizontal Ceiling/Floor Vents

All of the above leads to the following algorithm, called VENTCL, for calculating the flows V_{TOP} and V_{BOT} through horizontal ceiling/floor vents in an arbitrary Figure 1-configuration:

1. Calculate $\Delta\rho$ and Δp from Eqs. (1) and (2).
2. Calculate $V_{TOP,ST}$ and $V_{BOT,ST}$ from Eqs. (3)-(5).
3. If $\Delta\rho \leq 0$ then $V_{EX} = 0$ and V_{TOP} and V_{BOT} are calculated from Eq. (6). If $\Delta\rho > 0$ then:
4. Calculate $\Delta\rho_{FLOOD}$ from Eqs. (16) and (19).
5. Calculate V_{EX} from Eqs. (20) and (21).
6. Calculate V_{TOP} and V_{BOT} from Eq. (6).

The VENTCL algorithm is suitable for general use in zone-type compartment fire models.

6. Example Application of VENTCL: Steady-State Rate-of-Burning in a Ceiling-Vented Space

Consider a room containing a fire and fully-enclosed except for a circular or square horizontal ceiling vent. Refer to Figure 7. Assume steady-state conditions are achieved and that the environment in the room is relatively uniform with density, ρ , and with a greater-than-outside absolute temperature, T (i.e., $T_{BOT} = T$ and $\rho_{BOT} = \rho$), and with O_2 concentration by mass, μ . The environment outside the room is at uniform ambient conditions with density, absolute temperature, and O_2 concentration T_{AMB} , ρ_{AMB} , and μ_{AMB} , respectively (i.e., $T_{TOP} = T_{AMB}$ and $\rho_{TOP} = \rho_{AMB}$). For standard conditions, $\mu_{AMB} = 0.23$. The algorithm VENTCL can be used to estimate the steady rates-of-flow into and out of the room and then the steady-state burning rate, Q , that can be supported by the net rate of O_2 supplied by these flows.

Assume that the environment in the room can be modeled as a perfect gas which is identical to the outside environment. Then, since the absolute pressure is relatively uniform across the vent,

$$T/T_{AMB} \approx \rho_{AMB}/\rho \geq 1 \quad \text{and} \quad \Delta\rho = \rho_{AMB} - \rho \geq 0 \quad (22)$$

Assume further that the mass-flow rate of fuel introduced by the fire is negligible compared to the mass-flow-rate of the exchange-flow.

For steady state, conservation of mass in the room requires

$$\rho V_{\text{BOT}} = \rho_{\text{AMB}} V_{\text{TOP}} \quad (23)$$

Using Eq. (22) it follows from Eq. (23) that $V_{\text{BOT}} \geq V_{\text{TOP}}$. Therefore, according to Eq. (6) it is evident that: $\Delta p \geq 0$; $V_{\text{TOP,ST}} = 0$ and $V_{\text{BOT,ST}}$ are given by Eq. (3); and $V_{\text{TOP}} = V_{\text{EX}}$ and V_{BOT} are given by Eqs. (6) and (20).

Define

$$x = |\Delta p / \Delta p_{\text{FLOOD}}|^{1/2} \quad (24)$$

Using Eqs. (6), (3), and (20) in Eq. (23) leads to the following equations for x and V_{EX}

$$x^2 + \lambda x - 1 = 0 \quad (25)$$

$$V_{\text{EX}} = V_{\text{EX,MAX}}(1 - x^2) = V_{\text{EX,MAX}} \lambda x \quad (26)$$

where, for circular or square vents,

$$\lambda = C'_{\text{SHAPE}} (T/T_{\text{AMB}} + 1)^{1/2} / (T/T_{\text{AMB}} - 1) \quad (27)$$

$$C'_{\text{SHAPE}} = (10./2^{1/2}) C_D C_{\text{SHAPE}} (D/A_V^{1/2})^{5/2}$$

Taking $C_D = 0.68$ [1] and using Eq. (16) leads to

$$C'_{\text{SHAPE}} = \begin{cases} 4.5 & \text{for a circular vent} \\ 4.1 & \text{for a square vent} \end{cases} \quad (28)$$

The objective here is to find the energy-release rate, Q , of the fire in the room. This is related to the net mass-flow rate of O_2 which is added to the room by the vent flows and consumed in the combustion process. Using Eq. (23)

$$\begin{aligned} \text{Net rate of } O_2 \text{ consumed} &= \mu_{\text{AMB}} \rho_{\text{AMB}} V_{\text{EX}} - \mu \rho V_{\text{BOT}} \\ &= (1 - \mu/\mu_{\text{AMB}}) \mu_{\text{AMB}} \rho_{\text{AMB}} V_{\text{EX}} \end{aligned} \quad (29)$$

From [10]

$$C_{\text{OXYGEN}} = \text{rate of fire energy release/rate of } O_2 \text{ consumed} \quad (30)$$

$$= 13.2(10^3) \text{ kW}/(\text{kg}_{\text{OXYGEN}}/\text{s})$$

Using Eqs. (29) and (30) in Eq. (26) together with Eq. (21) leads to

$$Q^* = Q/[(1 - \mu/\mu_{\text{AMB}})\mu_{\text{AMB}}C_{\text{OXYGEN}}\rho_{\text{AMB}}(gA_v^{5/2})^{1/2}] = \quad (31)$$

$$0.28[(T/T_{\text{AMB}} - 1)/(T/T_{\text{AMB}} + 1)]^{1/2}(\lambda/2)x$$

The non-negative solution to Eq. (25) is

$$x = \{[(\lambda/2)^2 + 1]^{1/2} - (\lambda/2)\} \quad (32)$$

Using Eq. (30), $|\Delta p/\Delta p_{\text{FLOOD}}|$ and $Q/[(1 - \mu/\mu_{\text{AMB}})\mu_{\text{AMB}}C_{\text{OXYGEN}}\rho_{\text{AMB}}(gA_v^{5/2})^{1/2}]$ according to Eqs. (24) and (31), respectively, are plotted as a function of T/T_{AMB} in Figure 8. From these plots it is concluded that for circular or square vents and for realistic values of T/T_{AMB}

1. Q is dependent on vent area but is relatively insensitive to vent shape;
2. Q^* is relatively insensitive to T/T_{AMB} in the range $2. \leq T/T_{\text{AMB}}$, but is very sensitive to T/T_{AMB} in the range $1 \leq T/T_{\text{AMB}} \leq 2$;
3. Q^* actually reaches a maximum at $T/T_{\text{AMB}} = 5.8$ and 5.4 for circular and square vents, respectively; and
4. $|\Delta p/\Delta p_{\text{FLOOD}}|$ is always small.

Taking $\rho_{\text{AMB}} = 1.2 \text{ kg/m}^3$, $\mu_{\text{AMB}} = 0.23$, and using Eq. (30), Figure 8 was used to make the following estimates:

For $T/T_{\text{AMB}} = 2$, i.e., $T \approx 600\text{K}$, $Q/(1 - \mu/0.23) = 0.91(10^3)(A_v/\text{m}^2)^{5/4} \text{ kW}$, e.g., $Q/(1 - \mu/0.23) = 910\text{kW}$, 2.9kW , and 0.51kW for $A_v = 1.0\text{m}^2$, $1.0(10^{-2})\text{m}^2$, and $25.(10^{-4})\text{m}^2$, respectively.

For a given room temperature, the maximum O_2 consumption leading to the maximum possible steady-state burning rate, Q_{MAX} , will occur in fire scenarios where μ is near a characteristic extinction O_2 concentration, $\mu_{\text{EXTINCTION}}$.

For such scenarios, $Q/(1 - \mu/\mu_{AMB}) = Q_{MAX}/(1 - \mu_{EXTINCTION}/\mu_{AMB})$ and, as indicated, the plots of Figure 8 also yield estimates of Q_{MAX} . As an example, consider the combustion of methane or natural gas, and, according to Morehart and Zukoski [11], take $\mu_{EXTINCTION} \approx 0.13$. Then the above result is modified and it is concluded that

For $T/T_{AMB} = 2$, i.e., $T \approx 600K$, $Q_{MAX} = 0.40(10^3)(A_V/m^2)^{5/4}$ kW, e.g., $Q_{MAX} = 400kW$, $1.3kW$, and $0.22kW$ for $A_V = 1.0m^2$, $1.0(10^{-2})m^2$, and $25.(10^{-4})m^2$, respectively.

7. Acknowledgements

The author acknowledges gratefully the Naval Research Laboratory which sponsored this work under the technical management of Dr. Patricia A. Tatem and with the support of Ms. Jean L. Bailey.

8. References

- [1] Emmons, H., Vent Flows, Sect. 1/Chapter 8, SFPE Handbook of Fire Protection Engineering, SFPE, Boston, pp. 130-138, 1988.
- [2] Thomas, P.H., Hinkley, P.L., Theobald, C.R., and Simms, D.L., Investigations into the Flow of Hot Gases in Roof Venting, Fire Research Tech. Paper No. 7, Fire Research Station, Boreham Wood, Herts, UK, 1963.
- [3] Cooper, L.Y., Estimating the Environment and the Response of Sprinkler Links in Compartment Fires with Draft Curtains and Fusible Link-Actuated Ceiling Vents - Part I: Theory, NBSIR 88-3734, National Bureau of Standards, Gaithersburg, MD, 1988.
- [4] Hinkley, P.L., The Effect of Vents on the Opening of the First Sprinklers, Fire Safety J., 11, pp. 211-225, 1986.
- [6] Taylor, G. I., The Instability of Liquid Surfaces When Accelerated in a Direction Perpendicular to Their Planes. I, Proc. Roy. Soc., A, 201, pp. 192-196, 1950.
- [7] Epstein, M., Buoyancy-Driven Exchange Flow Through Small Openings in Horizontal Partitions, J. Heat Transfer, 110, pp. 885-893, 1988.
- [8] Brown, W.G., Natural Convection Through Rectangular Openings in Partitions - 2. Horizontal Partitions, Int. J. Heat Mass Transfer, 5, pp. 869-878, 1962.
- [9] Mercer, A. and Thompson, H., An Experimental Investigation of Some Further Aspects of the Buoyancy-Driven Exchange Flow Between Carbon Dioxide and Air Following a Depressurization Accident in a Magnox Reactor, Part 2: The Purging Flow Requirements in Inclined Ducts, J. British Nuclear Energy Soc., 14, pp. 335-340, 1975.
- [10] Huggett, C., Estimation of Rate of Heat Release by Means of Oxygen Consumption Measurements, Fire and Materials, 4, pp. 61-65, 1980.
- [11] Morehart, J.H. and Zukoski, E.E., Chemical Species Produced by Natural Gas Fires Near the Extinction Limit, California Institute of Technology October 1988 Quarterly Report to National Institute of Standards and Technology.

9. Nomenclature

A_V	vent area
C_D	vent flow coefficient
C_{OXYGEN}	Eq. (29)
C_{SHAPE}	vent shape factor, Eq. (14)
C'_{SHAPE}	vent shape factor, Eq. (27)
D	vent, pipe diameter; vertical vent depth
g	acceleration of gravity
P_{BOT}, P_{TOP}	pressure at bottom, top space, Figure 1
Q, Q_{MAX}	fire's burning rate and its maximum value
Q^*	dimensionless Q, Q_{MAX} , Eq. (31)
T, T_{AMB}	temperature of room gas, ambient
$V_{BOT, FLOOD}, V_{TOP, FLOOD}$	minimum volume-flow-rate from bottom, top for total purging
$V_{BOT, ST}, V_{TOP, ST}$	standard model volume-flow-rate from bottom, top
V_{EX}	volume-exchange-flow-rate
$V_{EX, MAX}$	maximum volume-exchange-flow-rate
V_{MEAS}	measured volume-flow-rate
W	length of backflow wedge
w	width of rectangular vent
x	$ \Delta p / \Delta p_{FLOOD} $, Eq. (24)
Δp	Eq. (1)
Δp_{FLOOD}	Δp for minimum totally-purging flows
$\Delta \rho$	Eq. (2)
λ	Eq. (27)
μ, μ_{AMB}	mass concentration of O_2 in the room, ambient

ρ, ρ_{AMB} density of room gas, ambient
 $\bar{\rho}$ Eq. (9)
 $\rho_{\text{BOT}}, \rho_{\text{TOP}}$ density at bottom, top
 ρ_{FLOOD} density of vent flow for totally-purging flows

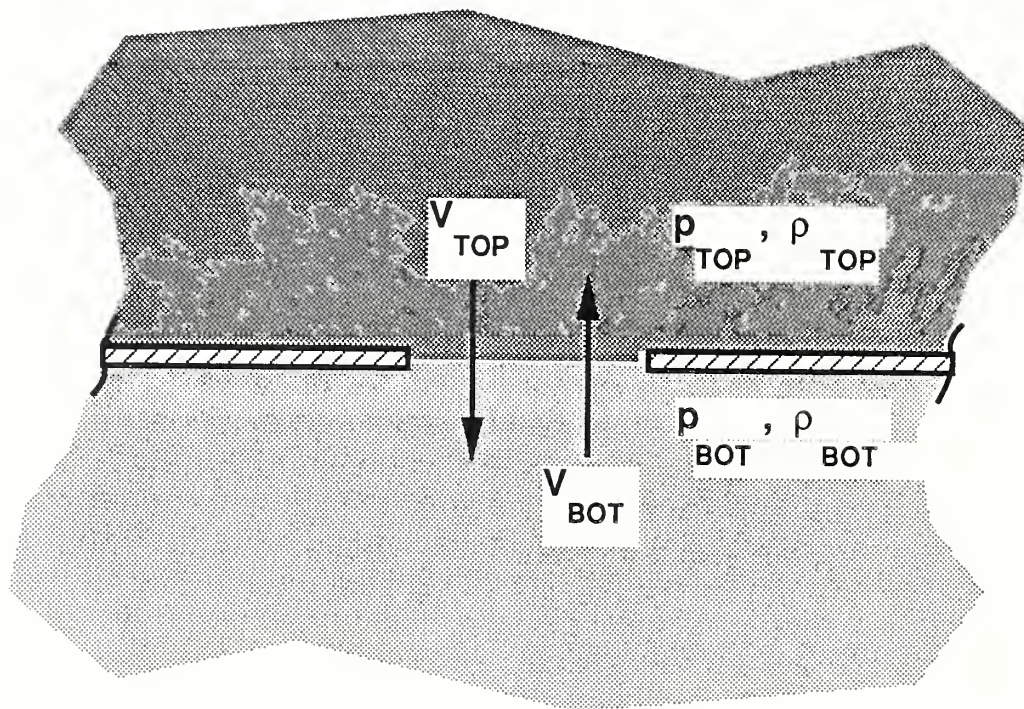
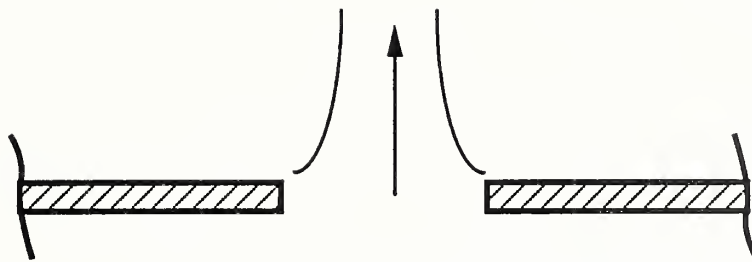


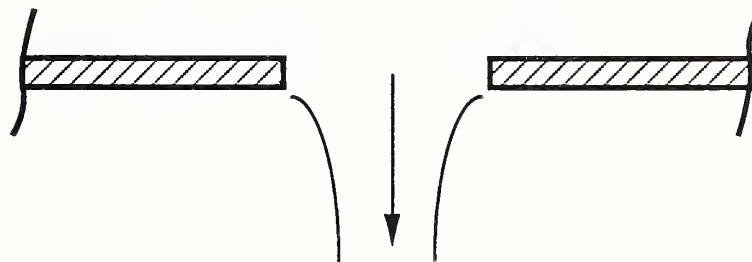
Figure 1. The basic horizontal-vent configuration.



(a) $\Delta p > 0 : V_{\text{TOP,ST}} = 0$



(b) $\Delta p = 0 : V_{\text{TOP,ST}} = V_{\text{BOT,ST}} = 0$



(c) $\Delta p < 0 : V_{\text{BOT,ST}} = 0$

Figure 2. The standard vent-flow model for horizontal vents.

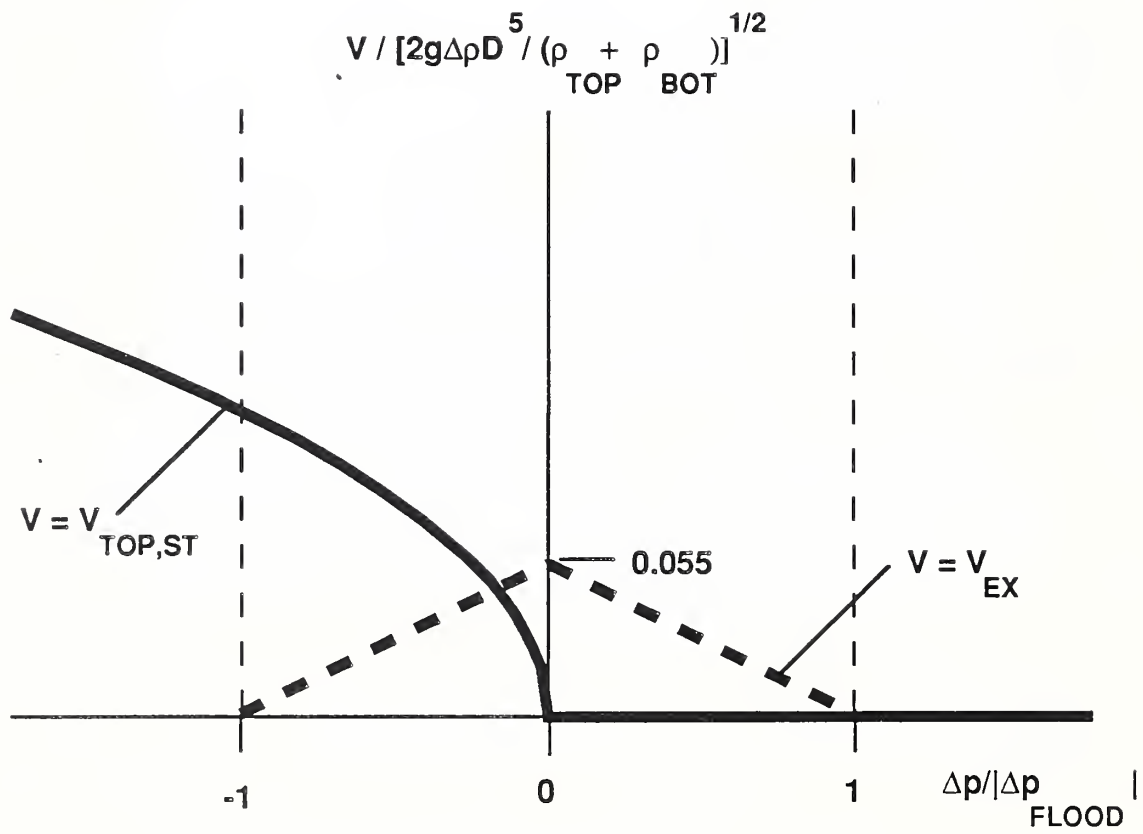


Figure 3. The volume-flow-rate components $V_{TOP,ST}$ and V_{EX} for unstable Figure-1 configurations, $\Delta\rho > 0$, plotted as functions of Δp .

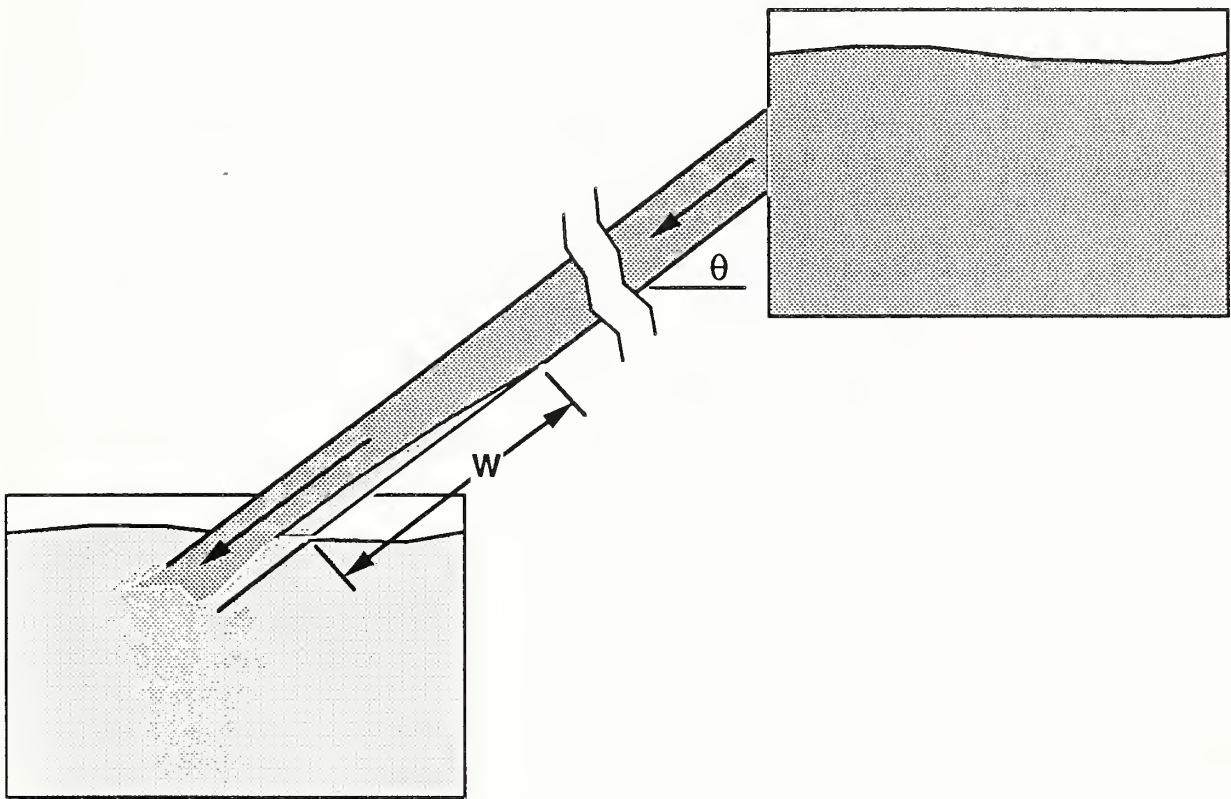


Figure 4. Sketch of the experimental setup of Mercer and Thompson [9].

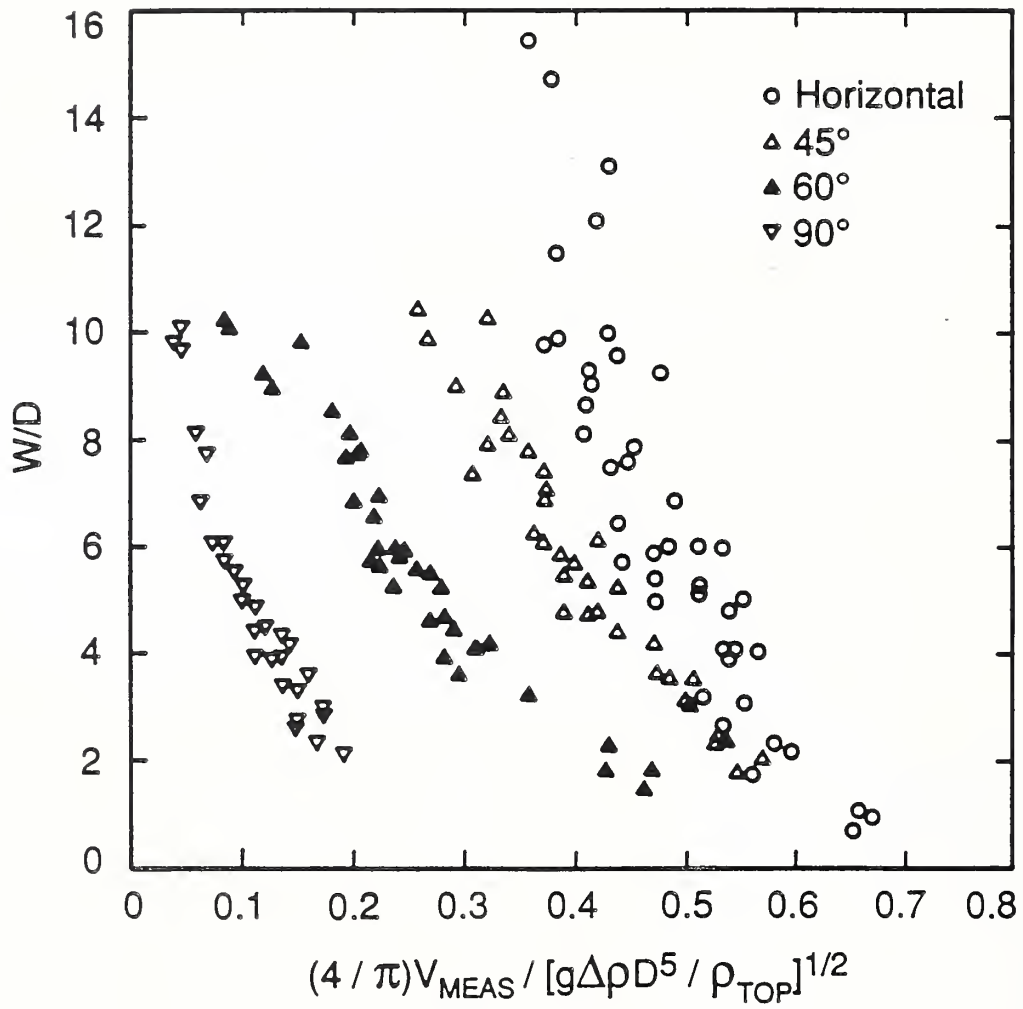


Figure 5. Plots of the Mercer and Thompson [9] data for $\theta = 0$ (horizontal), 45, 60, and 90° .

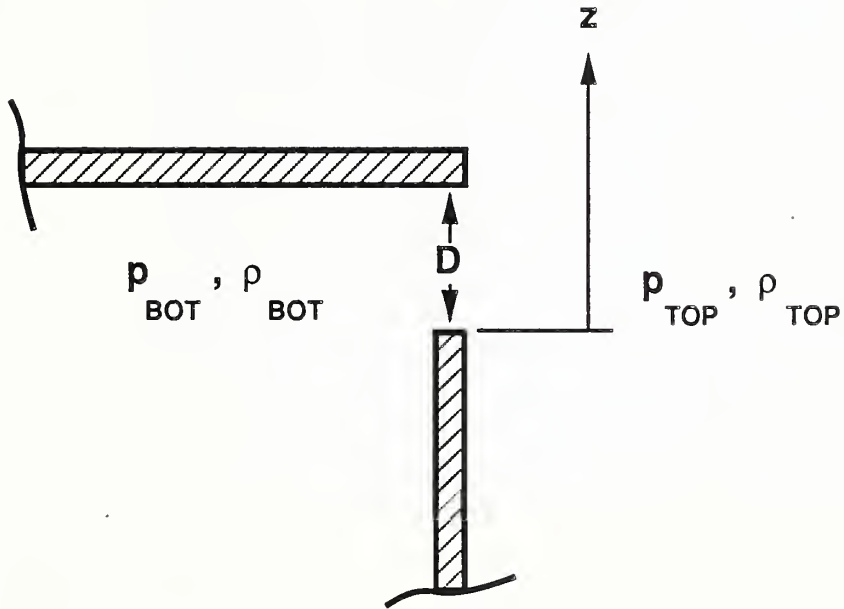


Figure 6. The vertical vent configuration used to calculate minimum totally-purging flow rates.

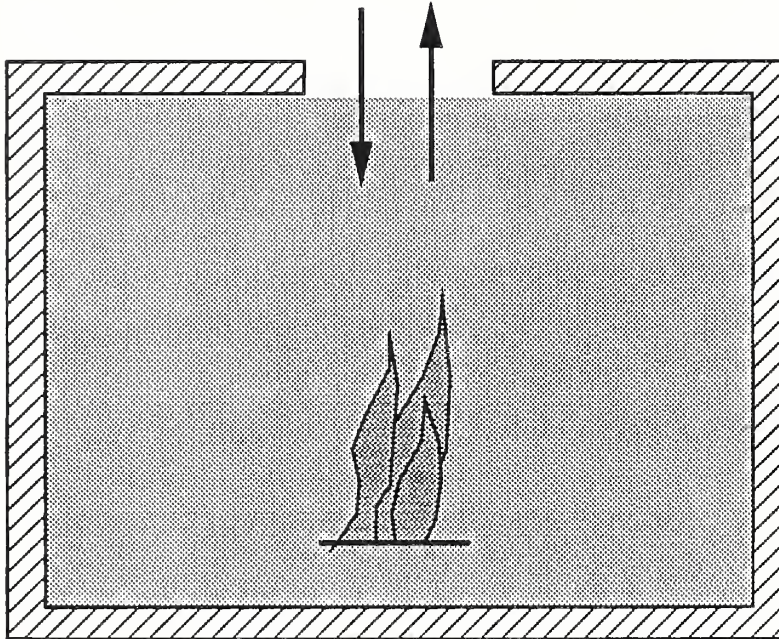


Figure 7. Configuration of a ceiling-vented room with a fire.

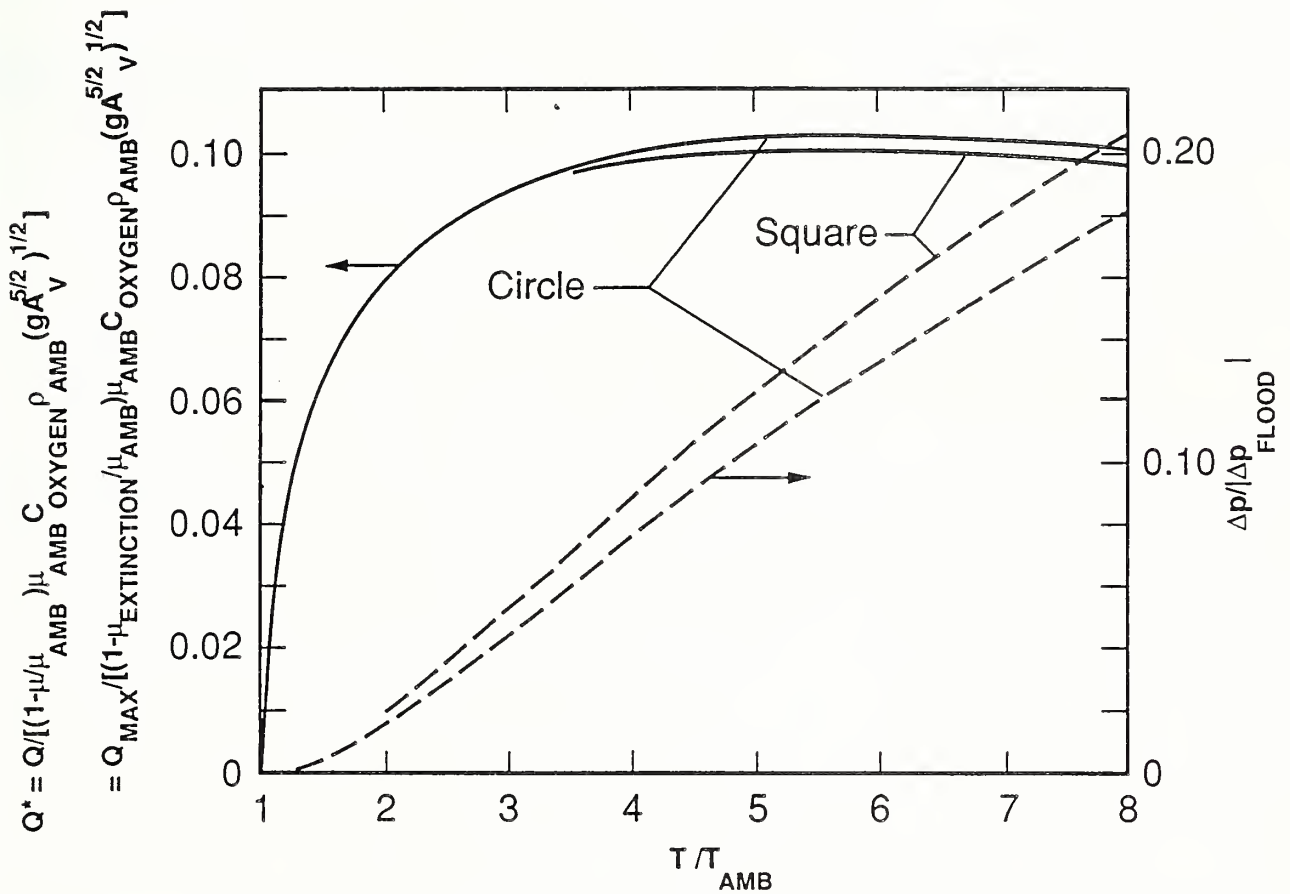


Figure 8. Plots of $\Delta p / \Delta p_{FLOOD}$, $Q / \left[(1 - \mu / \mu_{AMB})^{\mu_{AMB}} C_{OXYGEN} \rho_{AMB} (gA_V^{5/2})^{1/2} \right]$
 $= Q_{MAX} / \left[(1 - \mu_{EXTINCTION} / \mu_{AMB})^{\mu_{AMB}} C_{OXYGEN} \rho_{AMB} (gA_V^{5/2})^{1/2} \right]$ as
 functions of T / T_{AMB} for the configuration of Figure 7.

U.S. DEPT. OF COMM. BIBLIOGRAPHIC DATA SHEET (See instructions)	1. PUBLICATION OR REPORT NO. NIST-89/4052	2. Performing Organ. Report No.	3. Publication Date February 1989
4. TITLE AND SUBTITLE Calculation of the Flow Through a Horizontal Ceiling/Floor Vent			
5. AUTHOR(S) Leonard Y. Cooper			
6. PERFORMING ORGANIZATION (If joint or other than NBS, see instructions) NATIONAL INSTITUTE OF STANDARDS AND TECHNOLOGY NATIONAL BUREAU OF STANDARDS U.S. DEPARTMENT OF COMMERCE GAITHERSBURG, MD 20899		7. Contract/Grant No.	8. Type of Report & Period Covered
9. SPONSORING ORGANIZATION NAME AND COMPLETE ADDRESS (Street, City, State, ZIP) Naval Research Laboratory Washington, DC 20375			
10. SUPPLEMENTARY NOTES <input type="checkbox"/> Document describes a computer program; SF-185, FIPS Software Summary. is attached.			
11. ABSTRACT (A 200-word or less factual summary of most significant information. If document includes a significant graphy or literature survey, mention it here) Calculation of the flow through a horizontal vent located in a ceiling or floor of a multi-room compartment is considered. It is assumed that the environments of the two, vent-connected spaces near the elevation of the vent are of arbitrary relative buoyancy and cross-vent pressure difference, Δp . An anomaly of the standard vent flow model, which uses Δp to predict stable uni-directional flow according to Bernoulli's equation (i.e., flow rate is proportional to $\Delta p^{1/2}$), is discussed. The problem occurs in practical vent configurations of unstable hydrostatic equilibrium, where, for example, one gas overlays a relatively less-dense gas, and where $ \Delta p $ is relatively small. In such configurations the cross-vent flow is not uni-directional. Also, it is not zero at $\Delta p = 0$. Previously published experimental data on a variety of related flow configurations are used to develop a completely general flow model which does not suffer from the standard model anomaly. The model developed leads to a uniformly valid algorithm, called VENTCL, for horizontal vent flow calculations suitable for general use in zone-type compartment fire models. Based on an assumption of total consumption of inflowing oxygen, the algorithm is used in an example application where the maximum possible steady-state rate-of-burning in a ceiling-vented room is estimated as a function of room temperature and vent area.			
12. KEY WORDS (Six to twelve entries; alphabetical order; capitalize only proper names; and separate key words by semicolons) algorithms; building fires; compartment fires; computer models; computer programs; fire models; pressure differential; pressure effects; vent flow; zone models			
13. AVAILABILITY <input checked="" type="checkbox"/> Unlimited <input type="checkbox"/> For Official Distribution. Do Not Release to NTIS <input type="checkbox"/> Order From Superintendent of Documents, U.S. Government Printing Office, Washington, D.C. 20402. <input checked="" type="checkbox"/> Order From National Technical Information Service (NTIS), Springfield, VA. 22161		14. NO. OF PRINTED PAGES 30	15. Price \$12.95

